Anomalous effect due to oxygen vacancy accumulation below the electrode in bipolar resistance switching Pt/Nb:SrTiO3 cells

Shinbuhm Lee, Jae Sung Lee, Jong-Bong Park, Yong Koo Kyoung, Myoung-Jae Lee, and Tae Won Noh

Citation: APL Materials **2**, 066103 (2014); doi: 10.1063/1.4884215
View online: http://dx.doi.org/10.1063/1.4884215
View Table of Contents: http://scitation.aip.org/content/aip/journal/aplmater/2/6?ver=pdfcov
Published by the AIP Publishing

Anomalous effect due to oxygen vacancy accumulation below the electrode in bipolar resistance switching Pt/Nb:$SrTiO_3$ cells

Shinbuhm Lee,[1,2,a] Jae Sung Lee,[3,a] Jong-Bong Park,[4] Yong Koo Kyoung,[4] Myoung-Jae Lee,[5] and Tae Won Noh[1,2,b]

[1]*Center for Correlated Electron Systems, Institute for Basic Science, Seoul 151-747, Republic of Korea*
[2]*Department of Physics and Astronomy, Seoul National University, Seoul 151-747, Republic of Korea*
[3]*School of Physics, Korea Institute for Advanced Study, Seoul 130-722, Republic of Korea*
[4]*Analytical Science Group, Samsung Advanced Institute of Technology, Yongin, Gyeonggi-do 446-712, Republic of Korea*
[5]*Logic TD, Semiconductor R&D Center, Samsung Electronics, Hwaseong-si, Gyeonggi-do 445-701, Republic of Korea*

(Received 16 March 2014; accepted 9 June 2014; published online 19 June 2014)

In conventional semiconductor theory, greater doping decreases the electronic resistance of a semiconductor. For the bipolar resistance switching (BRS) phenomena in oxides, the same doping principle has been used commonly to explain the relationship between the density variation of oxygen vacancies ($V_o^{\cdot\cdot}$) and the electronic resistance. We find that the $V_o^{\cdot\cdot}$ density can change at a depth of ∼10 nm below the Pt electrodes in Pt/Nb:$SrTiO_3$ cells, depending on the resistance state. Using electron energy loss spectroscopy and secondary ion mass spectrometry, we found that greater $V_o^{\cdot\cdot}$ density underneath the electrode resulted in higher resistance, contrary to the conventional doping principle of semiconductors. To explain this seemingly anomalous experimental behavior, we provide quantitative explanations on the anomalous BRS behavior by simulating the mobile $V_o^{\cdot\cdot}$ [J. S. Lee *et al.*, Appl. Phys. Lett. **102**, 253503 (2013)] near the Schottky barrier interface. [http://dx.doi.org/10.1063/1.4884215]

The bipolar resistance switching (BRS) phenomenon is characterized by reversible and non-volatile resistance switching between bistable resistance states under electric fields.[1,2] Numerous applications have been proposed, including non-volatile memory.[3] Although the BRS mechanisms in many oxides remain controversial, it is commonly accepted that oxygen vacancies ($V_o^{\cdot\cdot}$ in the notation of Kröger and Vink[4]) should play an important role.[1–4] In conventional semiconductor theory, it is generally accepted that the electronic resistance of a semiconductor decreases with an increase in the density of defects.[5] For the BRS phenomenon in oxides, the same principle is used commonly to explain the relationship between the density variation of $V_o^{\cdot\cdot}$ and the electronic resistance.[1–4] Using the $V_o^{\cdot\cdot}$ model, researchers have explained many intriguing BRS phenomena successfully,[6,7] including the resistance state retention time, the switching speed, and the capability to withstand degradation. However, the $V_o^{\cdot\cdot}$ model also leaves many questions unanswered, because the real spatial distribution of $V_o^{\cdot\cdot}$ inside BRS oxides has rarely been investigated at the nanoscale.

Indeed, BRS phenomena involving $V_o^{\cdot\cdot}$ are difficult to investigate experimentally. In many BRS oxides, the current flow is localized to nanoscale conducting channels, so it is difficult to determine exactly where the resistance switching occurs.[2–4,7–9] In most cases, the quantity of $V_o^{\cdot\cdot}$ in typical

[a]S. Lee and J. S. Lee contributed equally to this work.
[b]Electronic mail: twnoh@snu.ac.kr

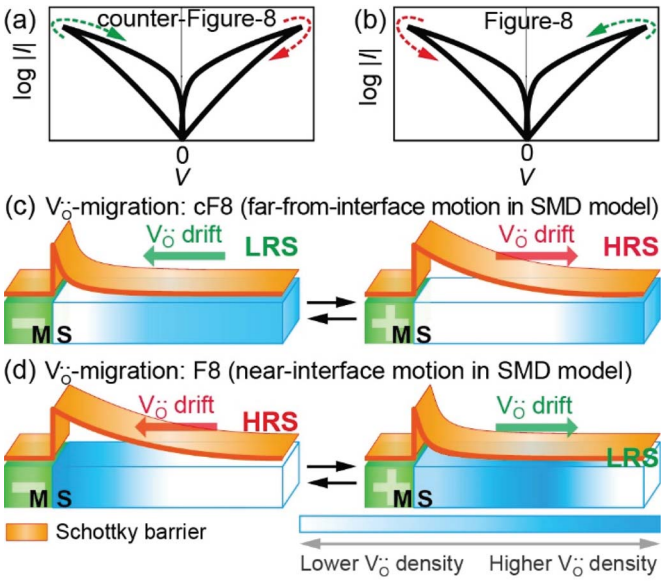

FIG. 1. SMD model of BRS phenomena. The mobile dopants are $V_o^{\cdot\cdot}$. (a) cf8 and (b) f8 *I–V* curves. (c) SMD model for cf8-type. The $V_o^{\cdot\cdot}$ move far from the interface. (d) SMD model for f8-type. The $V_o^{\cdot\cdot}$ move near the interface.

oxide thin films is quite low to be detected using direct imaging techniques, such as transmission electron microscopy (TEM).[10] In this study, we used Nb-doped $SrTiO_3$ (Nb:$SrTiO_3$) cells with Pt electrodes, which show BRS phenomena. We investigated the distribution of $V_o^{\cdot\cdot}$ using electron energy loss spectroscopy (EELS) and secondary ion mass spectrometry (SIMS). In the region of ~10 nm underneath the Pt electrodes, we observed that the $V_o^{\cdot\cdot}$ density of cells in the high-resistance state was much higher than in the low-resistance state. At first sight, this seems implausible, because it appears contrary to the conventional semiconductor doping principle. To explain this anomalous relationship, we carried out numerical simulations based on the "semiconductor with mobile dopants" (SMD) model. We found that the SMD model could explain the anomalous relationship between resistance changes and $V_o^{\cdot\cdot}$ distribution in Pt/Nb:$SrTiO_3$ cells. Our studies revealed how the change in $V_o^{\cdot\cdot}$ density under the electrode can influence the associated Schottky barrier and resistance changes.

Typical current–voltage (*I–V*) curves of BRS are pinched hysteretic loops.[1] Depending on the rotation direction, the hysteretic *I–V* curves are classified as either counter-figure-8 (cf8) or figure-8 (f8), as shown in Figs. 1(a) and 1(b), respectively. In the cf8 case,[1–3] low-to-high and high-to-low resistance switchings occur when positive and negative voltages are applied, respectively. However, in the f8 case,[11,12] low-to-high and high-to-low resistance switchings occur with opposite voltage polarities.

The rotation direction is an important criterion for judging valid physical models for BRS phenomena. For cf8-type,[1–3] most literature reports suggest an ionic model involving mobile $V_o^{\cdot\cdot}$ within interface and associated change of Schottky barrier. A negative (positive) voltage attracts (pushes) $V_o^{\cdot\cdot}$ to (away from) the interface, which induces decrease (increase) of the Schottky barrier width. For f8-type,[11,12] electronic models are proposed involving the trapping and detrapping of electrons at immobile $V_o^{\cdot\cdot}$ within interface. Each of these models can provide a simple explanation for each rotation direction. However, confusion arises because of several reports of the coexistence of both cf8- and f8-type curves in one sample.[13,14] To overcome these difficulties, a couple of explanations based on the homogeneity of $V_o^{\cdot\cdot}$ distribution in Fe-doped $SrTiO_3$ cells[13] and the position change of active Schottky interface in Pt/TiO_2/Pt cells[14] were proposed. However, these models may be applicable to the specific BRS material systems.

Most proposed BRS models in the field had been made with qualitative explanations, so that they mostly cannot provide quantitative comparison with experimental data.[1,2,4,9,13,14] To overcome these difficulties, we recently proposed the SMD model,[15] which simulates $V_o^{\cdot\cdot}$ distribution at a particular electric field by using the Monte Carlo method and calculates corresponding position-

dependent conduction band by solving the Poisson equations numerically. In the SMD model,[15] two rotation directions arise intrinsically, depending on how $V_o^{\cdot\cdot}$ are distributed inside an oxide cell. Consider a case where $V_o^{\cdot\cdot}$ are initially distributed primarily far from the Schottky interface. When $V_o^{\cdot\cdot}$ are attracted towards (repulsed from) the Schottky interface, as shown in Fig. 1(c), the Schottky barrier narrowed (widened), which induced a cf8 direction. Now, consider the other case, where the $V_o^{\cdot\cdot}$ are concentrated locally near the interface, as shown in Fig. 1(d). Then, the attraction and repulsion of the $V_o^{\cdot\cdot}$ distribution leads to the opposite modulation of the Schottky barrier, producing the f8 direction. That is, the SMD model predicts that more (less) doping will increase (decrease) the electronic resistance when the $V_o^{\cdot\cdot}$ are concentrated near the Schottky interface.[15] This seems to be contrary to the conventional theory of semiconductor doping. To confirm this anomalous behavior, it is important to obtain experimental evidence that the $V_o^{\cdot\cdot}$ distribution concentrated near the interface will actually result in the f8-type BRS. However, up to our best knowledge, no such experimental evidence has been reported previously.

We prepared Pt/Nb:$SrTO_3$ cells by putting Pt top and Ti bottom electrodes on 0.1 mm thick 0.5 wt.% Nb-doped $SrTiO_3$ (001) single crystals by sputtering. The Pt electrode has an area of $100 \times 100\,\mu m^2$ and a thickness of 40 nm. We selected the Pt/Nb:$SrTO_3$ cells for several reasons. First, most of our Pt/Nb:$SrTO_3$ cells had quite uniform electrical properties. Each virgin cell could only be used once in this study, because both EELS and SIMS are destructive methods. Thus, many cells with very similar electrical properties were required to minimize cell-to-cell variation. Our cells had excellent uniformity with the current values of 70 μA at 0.5 V with a standard deviation of 1%. Second, high-resistance state (HRS) and low-resistance state (LRS) currents in our Pt/Nb:$SrTO_3$ cells scaled with the electrode area.[4] This indicates that resistance switching occurs rather uniformly in the entire area under the electrode. Third, in our sample configuration of Pt/Nb:$SrTiO_3$/Ti, most resistance change should originate from only one place, namely, the Pt-Nb:$SrTiO_3$ interface. The Nb:$SrTiO_3$ single crystals should act as *n*-type semiconductors.[12] Metal-electrode/*n*-type semiconductor contacts were typically Ohmic in low-work-function metals (e.g., Ti has a work function of ∼4.2 eV) and Schottky-like rectifying in high-work-function metals (e.g., Pt, ∼5.2 eV).[12]

After forming, all of our Pt/Nb:$SrTiO_3$ cells exhibit f8-type *I*–*V* curves, as shown in Fig. 2(a). The resistance in the HRS at a readout voltage of 0.1 V was $\sim 10^7\ \Omega$ which is about a factor of ∼3 smaller than those of pristine cells. When we applied a positive voltage to the cells, their resistance decreased to $\sim 10^4\ \Omega$, to the LRS. When we applied a negative voltage to the devices in the LRS, the resistance recovered to $\sim 10^7\ \Omega$.

We used EELS techniques to investigate the existence of an accumulation layer of $V_o^{\cdot\cdot}$ very close to the Pt electrode.[10] Figure 2(b) shows O-*K* (O 1s → 2p, 532 eV) edge mapping images of the LRS (top) and HRS (bottom) cells. In the LRS cell, the bright spots, representing nearly stoichiometric oxygen atom occupancy, exist uniformly in the Nb:$SrTiO_3$ single crystal. However, in the HRS cell, the darker spots appear at a depth of ∼10 nm under the electrode. Since the contrast in the EELS images comes mostly from the pure intensity contrast, the dark spots represent deviations in oxygen atom occupancy from the ideal stoichiometry. Therefore, the $V_o^{\cdot\cdot}$ density just underneath the electrode of the HRS should be considerably higher than that of the LRS.

We also used SIMS to investigate the existence of high-density $V_o^{\cdot\cdot}$ very close to the interface of Pt/Nb:$SrTiO_3$ cells. SIMS is a sensitive tool for analyzing chemical elements at the surface region, down to ∼1–2 nm.[16] Figure 2(c) shows collected signals of secondary O^{2+} ions across the interface. As expected, the O^{2+} signal was much higher inside the Nb:$SrTiO_3$ single crystal than in the Pt electrode. The O^{2+} signal was enhanced at the interface of the LRS cell (dashed green line) and nearly flat in the HRS cell (solid red line). This O^{2+} signal enhancement was attributed to the oxygen exchange reaction,[4]

$$O_o \leftrightarrow \frac{1}{2}O_2 + V_O'' + 2e^-,$$

where O_o denotes oxygen ions in regular lattice sites. The difference in O^{2+} signal between the LRS and HRS cells indicates the existence of a large amount of mobile $V_o^{\cdot\cdot}$ at the interface of f8-type Pt/Nb:$SrTiO_3$ cells.

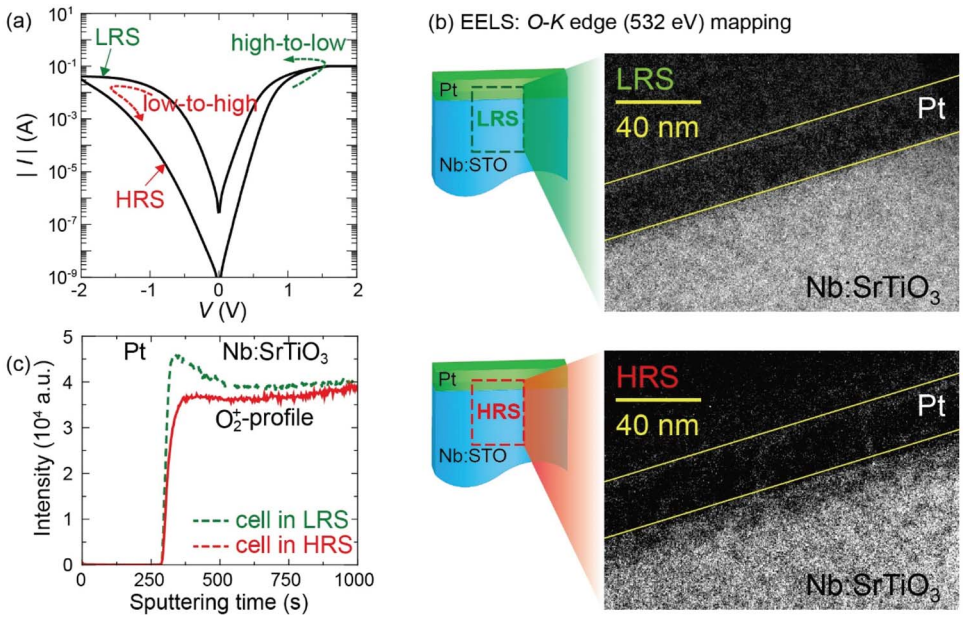

FIG. 2. (a) Experimental f8 *I–V* curves for a BRS Pt/Nb:$SrTiO_3$ cell. (b) EELS O-*K* (O 1s → 2p, 532 eV) edge mapping images of the LRS (upper) and the HRS (lower). (c) Collected SIMS signals for ejected secondary O^{2+} ions across the interface for a cell in the LRS (green dashed line) and the HRS (red solid line).

To explain the relation between $V_o^{\cdot\cdot}$ density distribution on the Schottky barrier and the resistance value, we used the SMD simulations. For the simulations, we considered a one-dimensional lattice with a lattice constant $a = 0.39$ nm and length $L = 80.34$ nm, as shown in Fig. 3(a). The Pt and Ti electrodes were in contact with the lattice at $x = 0$ and $x = L$, respectively. The contact between the Pt and the oxide layers is assumed to form a Schottky contact with a barrier height of 0.8 eV.[17] The contact between Ti and oxide layers is assumed to be Ohmic. We chose $L = 80.34$ nm instead of the actual Nb:$SrTiO_3$ single crystal thickness, 0.1 mm, since simulations with such a large size is practically infeasible. However, our simulations focusing on the Schottky interface region is expected to give tolerably correct results because most resistance change should originate from the Pt-Nb:$SrTiO_3$ interface as we mentioned earlier. In addition, we found that the slight change of the Schottky barrier height value strongly affects the final resistance. Therefore, all of the simulated results should be understood in a semi-quantitative level.

For the SMD simulations, we simulated the $V_o^{\cdot\cdot}$ distribution, $\rho_d(x)$, by assuming a simple hopping motion for mobile $V_o^{\cdot\cdot}$ as shown in Fig. 3(b).[15] The hopping barrier height U_o is assumed to be 1.01 eV.[4,13,14] Then, $\rho_d(x)$ becomes changed over time due to the hopping motion of $V_o^{\cdot\cdot}$ with $p_{+a}(x)$ and $p_{-a}(x)$, which are hopping probabilities for moving from x to $x + a$ and $x - a$, respectively. In order to make a more realistic model, we took into account of non-uniform electric field due to Schottky barrier in the hopping motion, which were not considered in our earlier model.[15] See Methods for the calculation and explicit forms of $p_{+a}(x)$ and $p_{-a}(x)$ and time evolution of $\rho_d(x)$.[18] For this study, we also took into account of the Joule heating effects, which is known to accelerate the hopping speed of $V_o^{\cdot\cdot}$.[7] The details of the Joule heating calculation are explained in the simulation methods section of the supplementary material.[18]

With the known $V_o^{\cdot\cdot}$ distribution, we calculated the position-dependent conduction band, $E_C(x)$, or the Schottky barrier from the solution of Poisson's equation:[5] $\nabla^2 E_C(x) = e(\rho_d(x) + \rho_e(x))/\epsilon$, where e is the electronic charge, ϵ is the permittivity of Nb:$SrTiO_3$ ($\epsilon = 300\epsilon_0$, ϵ_0 is the permittivity of air), and $\rho_e(x)$ is the density of electrons at each site x. The density of holes was assumed to be negligibly small compared with $\rho_d(x)$ and $\rho_e(x)$. The boundary conditions were $E_C(0) = 0.8$ eV and $E_C(L) = eV_{ext}$, where V_{ext} is the external voltage applied to the cell. To solve Poisson's equation, we used the self-consistent relaxation method.[15] The electrical current I was evaluated using the calculated $E_C(x)$. See simulation methods in the supplementary material for the calculation of I.[18]

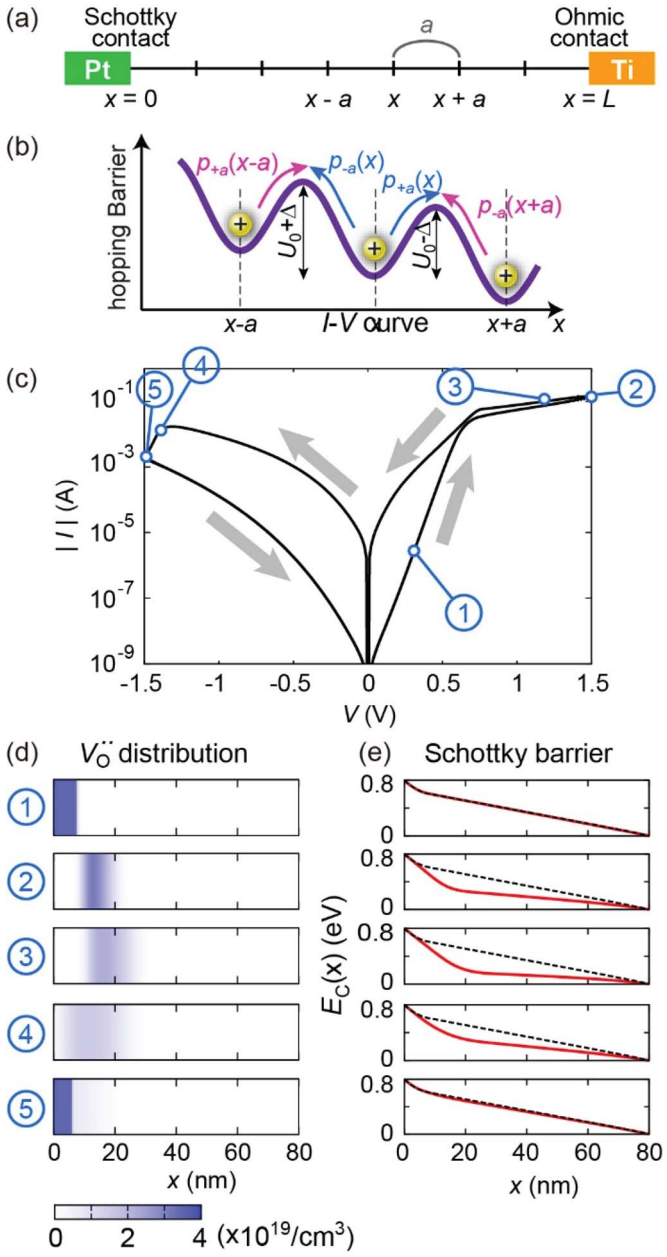

FIG. 3. Results of SMD model simulations. (a) Simple one-dimensional lattice used in the simulation. (b) Hopping probabilities for $V_o^{\cdot\cdot}$ to overcome a hopping barrier. (c) Simulated f8 *I–V* curve of a Pt/Nb:SrTiO$_3$ cell. (d) Calculated $V_o^{\cdot\cdot}$ redistribution across the sample. The numbers indicate each resistance state of the simulated f8 *I–V* curve. (e) Associated Schottky barrier changes coming from $V_o^{\cdot\cdot}$ redistribution.

To compare with our experimental results, we performed simulations by sweeping the applied voltage from -1.5 V $\rightarrow$ 1.5 V $\rightarrow$ -1.5 V with a voltage ramp rate of 1 V/s. To avoid the divergence problem, the maximum allowable concentration $\rho_{\max}$ of $V_o^{\cdot\cdot}$ was set to be 3.4×10^{19} cm^{-3}.[19,20] The variation of $\rho_{\max}$ does not affect the *I–V* polarity (see the supplementary material).[18] At the pristine state, the initial $V_o^{\cdot\cdot}$ distribution was assumed to be constant for all x: specifically, $\rho_d(x) = 3.4 \times 10^{18}$cm^{-3}. Then, we attracted $V_o^{\cdot\cdot}$ towards the Pt/Nb:SrTiO$_3$ interface to investigate the effect of oxygen vacancies near the interface. Our simulations generated an f8 *I–V* curve, as shown in Fig. 3(c). We also monitored the density change in mobile $V_o^{\cdot\cdot}$ at the interface and the associated Schottky barrier for each state (numbered resistance states, Fig. 3(c)), as shown in Figs. 3(d) and

3(e), respectively. The Schottky barriers in Fig. 3(e) were evaluated at $V_{ext} = 0$ with the following $V_o^{\cdot\cdot}$ distributions:

(1): In the HRS cell, $V_o^{\cdot\cdot}$ were accumulated near the interface.
(2)–(3): When we applied a positive voltage, positively charged $V_o^{\cdot\cdot}$ were repelled from the interface. High-to-low resistance switching occurred, and the Schottky barrier was narrowed.
(4)–(5): When we applied a negative voltage, $V_o^{\cdot\cdot}$ were attracted to the interface. Low-to-high resistance switching occurred, and the Schottky barrier was widened.

Note that the simulation results in Fig. 3(c) agree quantitatively with the experimental F8 *I–V* curve for our BRS Pt/Nb:$SrTiO_3$ cell, shown in Fig. 2(a). In addition, the $V_o^{\cdot\cdot}$ distributions were consistent with our experimental EELS and SIMS data, displayed in Figs. 2(b) and 2(c).

For an intuitive understanding, we summarize the physical meanings of the SMD simulation results as follows. When $V_o^{\cdot\cdot}$ are attracted to the interface and are concentrated highly near the interface, the other region becomes $V_o^{\cdot\cdot}$-deficient. Then, the $V_o^{\cdot\cdot}$-deficient region becomes more electronically resistive. When $V_o^{\cdot\cdot}$ increasingly migrate to the interface, the width of the $V_o^{\cdot\cdot}$-deficient region is widened, causing the overall cell resistance to rise to the HRS. Our simulation results demonstrate such a resistance change in the $V_o^{\cdot\cdot}$-deficient region in a semi-quantitative manner. As shown in Figs. 3(d) and 3(e), when the $V_o^{\cdot\cdot}$-deficient region is widened (narrowed), the electronic barrier for the $V_o^{\cdot\cdot}$-deficient region is raised (lowered), and widened (narrowed); thus, overall, the sample becomes more electronically resistive (conducting).

In summary, we investigated the existence of $V_o^{\cdot\cdot}$ underneath the electrodes in f8-type BRS Pt/Nb:$SrTiO_3$ cells using EELS and SIMS. We determined that $V_o^{\cdot\cdot}$ accumulated at a depth of ~10 nm under the electrode in HRS cells. The experimental results support the applicability of the SMD model, which we proposed recently, to mobile $V_o^{\cdot\cdot}$ in f8-type cells. Unlike previous models, the SMD model can describe the BRS phenomenon using one quantitative scheme. Our simulation will help to visualize the mechanism that occurs inside the BRS cell and will provide new insights into the control of material parameters for fabricating high-performance BRS memories.

This work was supported by the Research Center Program of the Institute for Basic Science (Grant No. EM1203) and the National Research Foundation of Korea (Grant No. NRF-2011-35B-C00014 to J.S.L.).

[1] D. B. Strukov, G. S. Snider, D. R. Stewart, and R. S. Williams, Nature (London) **453**, 80 (2008).
[2] J. J. Yang, M. D. Pickett, X. Li, D. A. A. Ohlberg, D. R. Stewart, and R. S. Williams, Nature Nanotech. **3**, 429 (2008).
[3] M.-J. Lee, C. B. Lee, D. Lee, S. R. Lee, M. Chang, J. H. Hur, Y.-B. Kim, C.-J. Kim, D. H. Seo, S. Seo, U.-I. Chung, I.-K. Yoo, and K. Kim, Nature Mater. **10**, 625 (2011).
[4] R. Waser, R. Dittmann, G. Staikov, and K. Szot, Adv. Mater. **21**, 2632 (2009).
[5] S. M. Sze, *Physics of Semiconductor Devices* (John Wiley and Sons, New York, 1981).
[6] D. B. Strukov and R. S. Williams, Appl. Phys. A **94**, 515 (2009).
[7] S. Menzel, M. Waters, A. Marchewka, U. Böttger, R. Dittmann, and R. Waser, Adv. Funct. Mater. **21**, 4487 (2011).
[8] J. P. Strachan, M. D. Pickett, J. J. Yang, S. Aloni, A. L. D. Kilcoyne, G. Medeiros-Ribeiro, and R. S. Williams, Adv. Mater. **22**, 3573 (2010).
[9] F. Miao, J. P. Strachan, J. J. Yang, M.-X. Zhang, I. Goldfarb, A. C. Torrezan, P. Eschbach, R. D. Kelley, G. Medeiros-Ribeiro, and R. S. Williams, Adv. Mater. **23**, 5633 (2011).
[10] D. A. Muller, N. Nakagawa, A. Ohtomo, J. L. Grazul, and H. Y. Hwang, Nature (London) **430**, 657 (2004).
[11] D.-J. Seong, M. Jo, D. Lee, and H. Hwang, Electrochem. Solid-State Lett. **10**, H168 (2007).
[12] T. Fujii, M. Kawasaki, A. Sawa, Y. Kawazoe, H. Akoh, and Y. Tokura, Phys. Rev. B **75**, 165101 (2007).
[13] R. Muenstermann, T. Menke, R. Dittmann, and R. Waser, Adv. Mater. **22**, 4819 (2010).
[14] F. Miao, J. J. Yang, J. Borghetti, G. Medeiros-Ribeiro, and R. S. Williams, Nanotechnology **22**, 254007 (2011).
[15] J. S. Lee, S. B. Lee, T. W. Noh, and B. Kahng, Appl. Phys. Lett. **102**, 253503 (2013).
[16] D. Briggs and M. P. Seah, *Auger and X-ray Photoelectron Spectroscopy* (John Wiley and Sons, New York, 1995).
[17] N. Ohashi, H. Yoshikawa, Y. Yamashita, S. Ueda, J. Li, H. Okushi, K. Kobayashi, and H. Haneda, Appl. Phys. Lett. **101**, 251911 (2012).
[18] See supplementary material at http://dx.doi.org/10.1063/1.4884215 for sample fabrication, measurement details, calculation for the hopping probabilities and electrical current, calculation method for the Joule heating, dependence of maximum value of oxygen vacancy concentration.
[19] M. Noman, W. Jiang, P. A. Salvador, M. Skowronski, and J. A. Bain, Appl. Phys. A **102**, 877 (2011).
[20] T. Baiatu, R. Waser, and K. H. Hardtl, J. Am. Ceram. Soc. **73**, 1663 (1990).